CORRECTIONS FOR ATMOSPHERIC AND ADJACENCY EFFECTS ON HIGH RESOLUTION SENSOR DATA -A CASE STUDY USING IRS-P6 LISS-IV DATA

Anu Rani Sharma, K.V.S.Badarinath and P.S. Roy

Atmospheric Science Section, National Remote Sensing Agency(Dept. of Space-Govt. of India), Balanagar, Hyderabad-500 037, India
Corresponding author: badrinath_kvs@nrsa.gov.in

KEY WORDS: IRS-P6, Aerosol, High Resolution, Reflectance, Classification.

ABSTRACT:

Path radiance due to aerosols plays an important role over satellite derived reflectance due to higher aerosol optical depth and their seasonal variations. In addition, satellite data from high-resolution sensors are subjected to adjacency effect, which reduces apparent surface contrast by decreasing the top of the atmosphere radiance over bright pixels and increasing the brightness of the dark pixels. In the present study, Second Simulation of Satellite Signal in the solar Spectrum (6S) radiative transfer model was used to analyze influence of atmospheric and adjacency affects over two different study areas corresponds to semi arid and tropical forest regions of India using IRS P6 – LISS-IV satellite data. Ground measurements of surface reflectance over selected crops were conducted to compare satellite derived surface reflectance. 6S model has been calibrated for local conditions using measurements on aerosol optical depth, water vapour and ozone parameters derived from MODIS-TERRA and OMI sensors. The methodology was applied for atmospheric correction of satellite data during intense biomass burning episodes in north-east region of India. Results of the study indicated that satellite reflectance measurements correlated well after correcting the satellite data for atmospheric effects using satellite based atmospheric parameters. Statistical information and seperability analysis over different land use categories suggested improved dynamic range and better seperability after atmospheric corrections. The major outcome of study suggested that atmospheric corrections using satellite derived atmospheric parameters provides a reasonably good data set when ground measurements on atmospheric parameters and surface reflectance are not available.

1. INTRODUCTION

A major constraint on the use of satellite imagery for both physical and empirical studies of the earth's surface lies in the degradation of the surface reflectance signal due to scattering and absorption by water vapour and aerosols in the atmosphere. In order to remove scattering and absorption effects and to derive precise surface reflectance from satellite image data, it is indispensable to apply the atmospheric correction.

Surface reflectance data obtained after atmospheric correction of satellite sensor imagery offers some advantages compared with usage of the original digital number (DN) or calibrated radiance data: (i) the interpretation of surface reflectance spectra is easier than the interpretation of DN spectra, which depend on atmospheric conditions and the solar illumination geometry, (ii) surface reflectance spectra can be compared with library or field spectra (Takashima et al.,2003) (iii) to compare and increase the scope of multi-sensor imagery, data must be calibrated to physical units (e.g. reflectance) as provided after atmospheric correction, (iv) the atmospheric scattering acts as a spatial low-pass filter causing a certain degree of blurring, which can be removed or at least strongly diminished with atmospheric correction (v) Effects of the sun position due to the recording time of day as well as seasonal differences are equalized (vi) Due to the quantitative analysis of the imagery, classification schemes developed once, can easily be applied to other subsequent recorded scenes because the reduced range of spectral object values (Richter et al., 2006).
A number of radiative transfer models, viz., LOWTRAN (Kneizys et al., 1988), MODTRAN (Berk et al., 1989), 5S (Tanre et al., 1990), 6S (Vermote et al., 1997b), SBDART (Ricchiazzi et al., 1998) and SMAC (Rahman et al., 1994) are available in literature. Amongst these models Second Simulation of Satellite Signal in the Solar Spectrum (6S) is the latest and sophisticated model with options for different satellite sensors (Tachiri, 2005).

In addition to the atmospheric effects, there exists a scattering effect due to the reflection of upward radiation coming from neighbouring pixels particularly in scenes with small heterogeneous irregular surfaced fields known as adjacency effect (Richter et al., 2006; Vermote et al., 2002).Adjacency effects reduce apparent surface contrast by decreasing the top of the atmosphere radiance over bright pixels and increasing the brightness of the dark pixels hence environment of the pixel should be taken into account in the atmospheric correction process (Richter et al., 2006;Vermote et al., 2002). In terms of a coarse spatial resolution, the adjacency correction is small and becomes highly significant for high spatial resolution sensors such as IRS-P6 LISS-IV (Sei, 2007). The common parameters required in these radiative transfer models include aerosol optical depth (AOD), water vapour, trace gases etc. Second Simulation of Satellite Signal in the Solar Spectrum (6S) model has the flexibility of using for variety of contemporary satellite sensors with options for carrying corrections for atmospheric and adjacency effects (Vermote et al., 1997b; Tachiri, 2005).
The objective of present study is to analyze the atmospheric and adjacency effects on IRS-P6 LISS-IV satellite data using 6S radiative transfer code. Ground reflectance measurements were carried out with spectroradiometer over two different crops viz. Maize and Sunflower over ICRISAT experimental farm located at Patancheru, Hyderabad, Andhra Pradesh. Surface reflectance retrieved from 6s code has been compared with top of atmosphere (TOA) reflectance and ground based Spectroradiometer measurements. The methodology was

validated on Mizoram state, north eastern India using satellite derived inputs on aerosol optical depth, ozone and water vapour.

2. STUDY AREA

The present study were carried out over two different regions viz.ICRISAT farm, Patancheru, Hyderabad(Study Area-1) and Mizoram state located in North-eastern part of India (Study Area-2). The study area-1 corresponding to International Crops Research Institute for the Semi-Arid Tropics (ICRISAT) was located in Patencheru (near Hyderabad), Andhra Pradesh state, India (17.5N, 78.5E; 545m (Figure 1). The semi-arid environment of the study area is characterized by high atmospheric water demand, a high mean annual temperature (>40°C); and a low, variable annual rainfall (400 to 1900 mm). The principal land cover types within the ICRISAT experimental farm include different crops and semi-arid grasslands.

The study area-2 of Mizoram is situated between Latitude 21°58' & 24° 35' N, Longitude 92° 15' & 93 ° 29', which is one of the Seven Sister States in north-eastern India on the border with Myanmar. Mizoram has the most variegated hilly terrain in the eastern part of India. The hills are steep (avg. height 1000 meters) and separated by rivers which flow either to the north or south creating deep gorges between the hill ranges. Mizoram has a mild climate: it is generally cool in summer and not very cold in winter. During winter, the temperature varies from 11°C to 21°C and in summer it varies between 20°C to 29°C. The entire area is under the regular influence of monsoons. It rains heavily from May to September and the average rainfall is 254 cm, per annum.30% of Mizoram is covered with wild bamboo forests, and faces severe threat due to shifting cultivation (locally known as 'Jhum') and increasing population. The natural jhum cycle, which used to be 5-6 years, has reduced to 2-3 years because of increasing population resulting in the conversion of primary forests to secondary forests and deciduous systems with a subsequent loss of biodiversity.

Figure 1: Location map of study area.

3. METHODOLOGY

Ground based measurements for spectral reflectance over Maize and Sunflower crops were conducted with Field Spec Pro Spectroradiometer at ICRISAT Farm near Hyderabad, Andhra Pradesh, India on 24th January, 2007. The Spectroradiometer operates in the spectral range of 350 nm to 2500 nm covering visible, near IR and short wave spectral regions and has a spectral sampling interval of 1.0 nm

Spectral reflectance data over Maize and Sunflower crops in 350 to 2500 nm ranges at 1 nm interval were collected using spectroradiometer. The spectroradiometer was operated vertically one meter above each canopy. The average reflectance of ten measurements over each canopy was used to estimate the mean reflectance. The reflectance data ρ (λ) of spectroradiometer was converted to LISS- IV sensor's different bands using the spectral response function (S_i (λ)) of the LISS-IV sensor's bands (i), as

$$\text{LISS-IV } \rho(\lambda_i) = \frac{\int \rho(\lambda)\, S_i(\lambda)\, d\lambda}{\int S_i(\lambda)\, d\lambda} \quad (1)$$

In order to estimate surface reflectance from satellite data in the solar radiation wavebands, the conversion of digital numbers to reflectance data is achieved in three steps (1) radiance conversion, (2) apparent reflectance conversion and (3) atmospheric correction.

Radiance conversion of digital numbers can be achieved using sensor calibration coefficients. Digital number (DN) of satellite data was converted into spectral radiance (L_i) using pre launch calibration coefficients then the top of atmosphere (TOA) reflectance (ρ (λi)) for each spectral bands were computed by converting spectral radiance to reflectance as,

$$\rho_{\lambda i} = \frac{\pi L i\, d^2}{E_o \cos\theta} \quad (2)$$

Where, L_i is spectral radiance, d^2 is Earth–Sun distance, E_0 is the ex-atmospheric solar irradiance, θ is the solar zenith angle. Further the surface reflectance free from atmospheric effects is computed as (Mahiny and Turner, 2007), using 6S model which predicts the reflectance of the objects at the top of atmosphere using surface reflectance and atmospheric condition information (Vermote et al 2006).

$$\text{Reflectance } (\rho_s) = \frac{[(A_\rho + B)]}{[1 + (\gamma\ (A_\rho + B))]} \quad (3)$$

Where A= 1/αβ , B = -ρ / β and p = TOA reflectance,α is the global gas transmittance, β is the total scattering transmittance, ϒ is the spherical albedo and ρ is the atmospheric reflectance. The input parameters on solar zenith and azimuth angle, satellite zenith and azimuth angle, date and time of image acquisition required for 6S model, were extracted from LISS-IV Header file supplied along with satellite data. Aerosol optical depth (AOD) at 550 nm data from MOD04 Level-2 at 10x10 km resolution (http://ladsweb.nascom.nasa.gov/data), water vapour from MOD08_M3.005 products (http://g0dup05u.ecs.nasa.gov/Giovanni/) and columnar ozone data from L3_Ozone_OMI

products(ftp://toms.gsfc.nasa.gov/pub/OMI/data /data/ozone) were used in 6S code for atmospheric corrections.

The final step in atmospheric correction algorithm was the removal of the image blurring caused by those photons reflected by the target environment and scattered by the atmospheric particles into the sensor's line of sight. This effect is called adjacency effect because the apparent signal at the TOA of a pixel comes also from adjacent pixel and is very important in high resolution sensors such as LISS-IV.The correction for adjacency effect involves inverting the linear combination of reflectances to isolate the reflectance of the target pixel (Guanter et al., 2007). The formulation (Equation-3) proposed by (Vermote et al. 1997b), weighting the strength of the adjacency effect by the ratio of diffuse to direct ground-to-sensor transmittance, was used:

$$\rho_s = \rho_s^{\mu} + \frac{t_d}{e^{-\tau/\mu_v}}\left[\rho_s^{\mu} - \bar{\rho}\right] \quad (4)$$

Where ρ_s^{μ} is the surface reflectance before the adjacency treatment, ρ_s is the final surface reflectance, output of the complete atmospheric correction algorithm, μ_v is the cosine of the View zenith angle and $\bar{\rho}$ is the average of the environment reflectance.

4. RESULTS AND DISCUSSIONS

Figure 2 shows 03rd February 2007 IRS-P6 LISS-IV false color composite before and after atmospheric correction over the study area of ICRISAT experimental farm. The improvement in contrast between various features with edges between features could be noticed in Figure 2c after correcting the satellite data for atmospheric and adjacency effects. Figure 2(d) and 2 (e) shows enlarged view of parts of study area suggesting sharpening of edges between crop fields after atmospheric and adjacency correction.

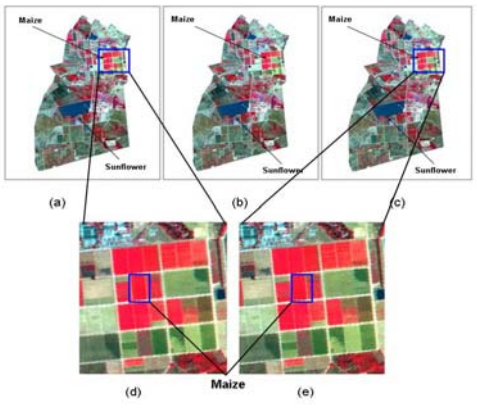

Figure 2: IRS-P6 LISS-IV false color composite (FCC) of the study area (a) uncorrected, (b) corrected for atmospheric effects and (c) corrected for atmospheric and adjacency effects. Enlarged portion of part of study area (d) uncorrected (e) corrected for atmospheric and adjacency effects.

Figure 3 (a-b) shows ground measured surface reflectance in different bands of IRS-P6 LISS-IV and NDVI comparison over Maize and Sunflower crop respectively measured in the study area of ICRISAT farm. The patterns in ground reflectance, 6s corrected reflectance and adjacency corrected reflectance are similar and the data values match with ground observations after atmospheric corrections. Comparison of NDVI derived from LISS-IV before and after corrections suggested that NDVI values over maize and sunflower crop are close to ground measured values. Further comparison of NDVI derived from LISS-IV before and after corrections suggested that NDVI values over maize and sunflower crop are close to ground measured values. NDVI values from LISS-IV data after atmospheric and adjacency correction over maize and sunflower crops were 0.62 & 0.55 respectively and are closer to ground measured NDVI of 0.69 & 0.58 compared to uncorrected data values of 0.47 & 0.4. For Maize crop NDVI showed increase of 25% whereas for Sunflower crop it showed increase of 26% after atmospheric correction.

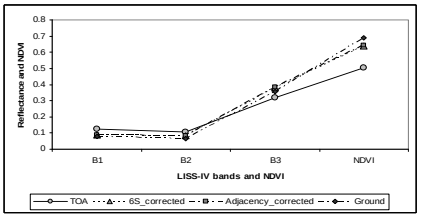

(a)

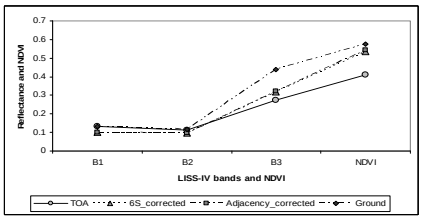

(b)

Figure 3 (a-b) Surface reflectance in different bands of IRS-P6 LISS-IV and NDVI comparison over (a) Maize (b) Sunflower crop.

Significant difference between uncorrected TOA reflectance and ground observed reflectance and matching of ground reflectance observations of Maize and Sunflower crops with 6S corrected reflectance suggested towards importance of atmospheric and adjacency correction to satellite data where atmospheric aerosols plays an important role in attenuating satellite signal. Further for validation of atmospheric correction methodology study area-2 of Mizoram, situated in North – eastern India was selected. MODIS derived aerosol optical depth, water vapour and AURA – OMI derived ozone were used in the radiative transfer model for correcting the IRS-P6 LISS-IV high satellite data.

Mizoram state had higher incidence of forest fires during March, 2006 due to slash-and-burn agricultural practices and clearing of bamboo flowering pockets. (Badarinath et al., 2007). Figure 4 (a-c) shows the IRS-P6 – LISS IV, false colour composites (FCC) (a) before correction (b) after atmospheric correction (c) after atmospheric and adjacency correction on 16 March, 2006 over a part of Lunglei District of Mizoram state. Due to higher incidence of forest fires total valley of Mizoram state was covered by smoke plumes and obstructed the landscape features delineation in satellite imagery. The landscape features (i.e. shifting cultivation patches) covered by smoke plumes due to

forest fires in FCC of IRS-P6 – LISS IV sensor are clearly visible after atmospheric and adjacency corrections.

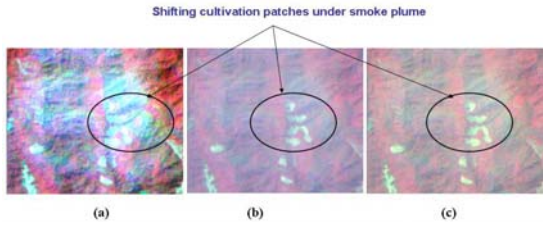

Figure 4 (a-c): IRS-P6 – LISS IV, (FCC) (a) before correction (b) after atmospheric correction (c) after atmospheric and adjacency correction.

Figure 5 shows the histograms of TOA reflectance and atmospherically corrected reflectance for Green, Red and NIR bands of IRS-P6 LISS-IV satellite data over parts of study area. Reduction in reflectance values and histograms shift towards origin were observed in green and red bands after atmospheric and adjacency correction. This was attributed to contribution of atmospheric Rayleigh and aerosol scattering in the shorter wavelength visible spectral bands. Correcting the atmospheric effects tends to decrease the reflectance values and introduce significant variations in the spectral reflectances in atmospherically corrected versus un-corrected spectral bands. The reflectance values in the NIR band increased after the atmospheric correction. This is due to lesser influence of aerosols and air molecules in NIR region. However, the atmospheric absorption due to water vapour, carbon dioxide, methane and other gases can have significant role in the NIR region. (Vermote et al., 2006).

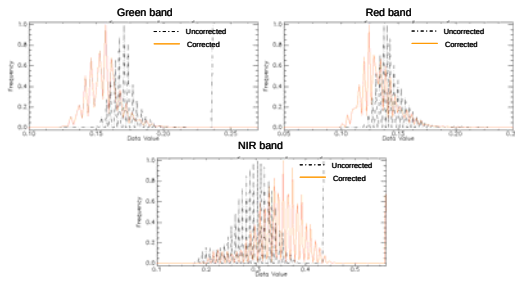

Figure 5: Histograms of TOA reflectance and atmospherically corrected reflectance for Green, Red and NIR bands.

Figure 6 shows co spectral parallelepiped or ellipse plot in two dimensional feature space over different land cover classes in green vs. NIR band combination for uncorrected and 6S model derived reflectance values. It can be seen clearly from the figure that atmospherically corrected reflectance showed increased seperability between the features compared to uncorrected reflectance (Song et al., 2001: Jain, 1989). The digital separability measures also showed improvement in separability between various land use/land cover features after corrections.

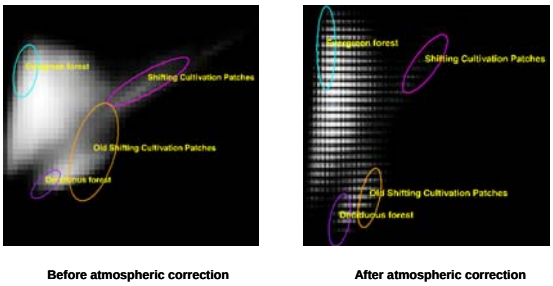

Figure 6: Seperability analysis before and after atmospheric correction for Green: NIR band combination.

Table 1 lists the basic statistics: minimum, maximum, mean, and standard deviation for each band of LISS-IV total image before, after atmospheric correction and after adjacency correction.

The standard deviation is higher for adjacency corrected reflectance, comparatively less for atmospherically corrected reflectance and lowest for uncorrected image for each band of LISS-IV, which indicates improvement in information content (Lu et al., 2004; Hashim et al., 2004) after atmospheric and adjacency correction. Decrease in minimum value and increase in maximum value of histogram for all spectral bands after atmospheric and adjacency correction suggests improvement in dynamic range.

5. CONCLUSIONS

We have evaluated the potential of 6S radiative transfer model for atmospheric and adjacency corrections for IRS-P6 LISS-IV high spatial resolution sensor over semi arid and tropical regions of India where atmospheric aerosols plays a major role In attenuating satellite signals. Ground reflectance measurements correlated well with satellite derived reflectance values corrected for atmospheric effects using 6S model. Satellite derived input parameters on aerosol optical depth, water vapour and ozone provide scope for operational atmospheric corrections of satellite data. Results of the study suggested significant increase in contrast and greater improvement in image visualization in areas with high aerosol loading due to forest fires. Statistical methods on seperability analysis over different land use categories suggested improvement in dynamic range and seperability between features after atmospheric and adjacency correction.

REFERENCES

Badarinath, K.V.S., Kharol, S. K. and. Kiran Chand, T.R., 2007.Use of satellite data to study the impact of forest fires over the northeast region of India. IEEE-GRSL, 4, pp. 485-489.

Berk, A., Bernstein, L. S., and Robertson, D. C, 1989.MODTRAN: A Moderate Resolution Model for LOWTRAN 7. GL-TR-89- 0122. Phillips Lab., Hanscom Air Force Base, Mass.

Guanter, L., Sanpedro, G., Carmen, M. D., and Moreno, J., 2007.A method for the atmospheric correction of ENVISAT / MERIS data over land targets. International Journal of Remote Sensing, 28, pp.709 – 728.

Hashim, M., Watson, A. and Thomas, M., 2004, An approach for correcting inhomogeneous atmospheric effects in remote sensing images, International Journal of Remote Sensing, 25(22), pp. 5131 – 5141.

Jain, A. K., 1989.Fundamentals of Digital Image Processing, Englewood Cliffs, NJ: prentice- Hall, pp.418-421

Kneizys, F. X., Shettle, E. P., Abreu, L. W., Chetwynd, J. H., Anderson, G. P., Gallery, W. O., Selby, J. E. A., and Clough, S. A.,1988.User's guide to LOWTRAN 7, Air Force Geophysics Laboratory, Hanscom AFB Environmental Research Report ERP, No.1010.

Lu, D., Mausel, P., Brondizio, E. and Moran, E., 2004.Assessment of atmospheric correction methods for Landsat TM data applicable to Amazon basin LBA research, International Journal of Remote Sensing, 23, pp. 2651 – 2671.

Mahiny, A. S., and Turner, B. J., 2007. A comparison of four common atmospheric correction methods. Photogrammetric Engineering & Remote Sensing, 73, pp. 361-368.

Rahman, H., and Dedieu, G., 1994.SMAC: A simplified method for atmospheric correction of satellite measurements in the solar spectrum, International Journal of Remote Sensing, 15, pp. 123–143.

Ricchiazzi, P., Yang, S., Gautier, C., and Sowle, D., 1998.SBDART: A Research and Teaching Software Tool for Plane-Parallel Radiative Transfer in the Earth's Atmosphere, Bulletin of the American Meteorological Society, 79(10), pp. 2101–2114.

Richter, R., Schlapfer, D., and Muller, A. 2006. An automatic atmospheric correction algorithm for visible/NIR imagery, International journal of remote sensing.27, pp.2077–2085.

Sei, A., 2007.Analysis of adjacency effects for two Lambertian half-spaces, International Journal of Remote Sensing, 28, pp. 1873 – 1890.

Song, C., Woodcock, C. E., Soto, K. C. Lenney, M. P., and Macomber, S. A.,2001. Classification and change detection using Landsat TM Data: When and How to Correct Atmospheric Effects, Remote Sensing of Environment, 75, pp.230-244.

Tachiri, K., 2005. Calculating NDVI for NOAA/AVHRR data after atmospheric correction for extensive images using 6S code: A case study in the Marsabit District, Kenya, ISPRS Journal of Photogrammetry & Remote Sensing, 59, pp. 103–114.

Takashima, T., Rathbone, C., and Clementson , L., 2003. Atmospheric correction of SeaWiFS ocean color data in the southern hemisphere. Applied Mathematics and Computation, 141, pp. 241 – 259.

Tanre, D., Deroo, C., Dahaut,P., Herman, M., and Morcrette, J. J.,1990.Description of a computer code to simulate the satellite signal in the solar spectrum: the 5S code, International Journal of Remote Sensing, 11, pp. 659–688.

Vermote, E. F., and Saleous N. Z., Operational atmospheric correction of MODIS visible to middle infrared land surface data in the case of an infinite lambertian target, 2006. In: Earth Science Satellite Remote Sensing, Science and Instruments, (eds: Qu. J. et al), l, pp. 123 – 153.

Vermote, E. F., Saleous, N. Z., and Justice, C. O. 2002.Atmospheric correction of MODIS data in the visible to middle infrared: first results," Remote Sensing of Environment, 83, pp. 97– 111.

Vermote, E. F., Tanre, D., Deuze, Herman, M. and Morcrette, J., 1997b.Second simulation of the satellite signal in the Solar Spectrum, 6S: An overview.IEEE Transactions on Geoscience and Remote Sensing, 35, pp. 675-686.

ACKNOWLEDGEMENTS

The author wishes to thank Director (NRSA), for necessary help and continuous encouragement.

	Uncorrected			**Atmospherically corrected**			**Adjacency corrected**		
	Green	**Red**	**NIR**	**Green**	**Red**	**NIR**	**Green**	**Red**	**NIR**
Minimum	0.144	0.111	0.162	-0.113	-0.070	-0.039	-0.228	-0.149	-0.106
Maximum	0.236	0.284	0.437	0.255	0.324	0.519	0.3790	0.379	0.562
Mean	0.170	0.143	0.293	0.150	0.129	0.333	0.1068	0.129	0.333
Standard deviation	0.008	0.012	0.036	0.045	0.037	0.076	0.047	0.038	0.077

Table 1: Statistical values associated with uncorrected and corrected image